Electrical stimulation of low-threshold afferent fibers induces a prolonged synaptic depression in lamina II dorsal horn neurons to high-threshold afferent inputs in mice

Andrei D. Sdrulla[a,*], **Qian Xu**[b,c,*], **Shao-Qiu He**[a], **Vinod Tiwari**[a], **Fei Yang**[a], **Chen Zhang**[a,d], **Bin Shu**[a], **Ronen Shechter**[a], **Srinivasa N. Raja**[a], **Yun Wang**[d], **Xinzhong Dong**[b,c], and **Yun Guan**[a,†]

[a]Department of Anesthesiology and Critical Care Medicine, Johns Hopkins University, School of Medicine, Baltimore, Maryland, 21205

[b]The Solomon H. Snyder Department of Neuroscience, Center for Sensory Biology, Johns Hopkins University, School of Medicine, Baltimore, Maryland, 21205

[c]Howard Hughes Medical Institute, Johns Hopkins University, School of Medicine, Baltimore, Maryland, 21205

[d]Department of Anesthesiology, Beijing Chaoyang Hospital, Capital Medical University, Beijing 100020, China

Summary statement

This study suggests that electrical stimulation of low-threshold Aβ-fibers induces prolonged inhibition of excitatory postsynaptic current evoked by high-threshold afferent inputs in lamina II neurons.

Keywords

Aβ-fiber; neurostimulation; substantia gelatinosa; neuropathic pain; evoked postsynaptic currents

1. Introduction

Chronic pain has reached epidemic proportions worldwide. Despite significant efforts to develop new pharmacologic agents, chronic neuropathic pain remains difficult to treat with current medications [13]. Electrical stimulation of low-threshold afferent Aβ-fibers (Aβ-ES), which mostly signal non-noxious inputs, is used clinically for treating neuropathic pain

conditions that are refractory to pharmacotherapy. These therapies include transcutaneous electrical nerve stimulation (TENS), certain forms of peripheral nerve stimulation (PNS), and spinal cord stimulation (SCS), which activates Aβ-fibers in the dorsal column. Neurostimulation therapies provide important alternative strategies for treating chronic pain conditions when other therapies have failed or produce side effects that substantially impair a patient's quality of life [12,15,45]. The premise behind using Aβ-ES for pain treatment arose from the "gate control" theory, whereby activity of low-threshold afferent fibers triggers pain inhibitory mechanisms in the spinal cord [30]. However, details about the spinal neuronal substrates and cellular mechanisms that underlie pain inhibitory effects of Aβ-ES remain elusive [15,16].

High-threshold afferent fibers (C-, Aδ-fibers) mostly transmit noxious information and terminate principally at superficial (I/II) dorsal horn in the spinal cord. The superficial dorsal horn serves as both a relay station for ascending pain signaling and an important site for integration and modulation of converging nociceptive information. In particular, substantia gelatinosa (SG, lamina II) neurons form important local inter-neuronal circuitry that modulates spinal nociceptive transmission and may be essential for Aβ-ES-induced analgesia [11]. However, it is unclear how Aβ-ES modulates synaptic responses to noxious inputs in superficial dorsal horn. Although previous studies have described different forms (e.g., potentiation, depression) of synaptic plasticity in superficial dorsal horn, the conditioning stimulation used in those studies often requires high intensities that activate high-threshold afferent fibers [29,38,41,42]. To our knowledge, no reports have examined whether conditioning paradigms that use low-threshold Aβ-fiber intensities are capable of inhibiting high-threshold synaptic transmission (presumably nociceptive) in superficial dorsal horn neurons. Therefore, the central effects of Aβ-ES on excitability of SG neurons are largely unknown, especially after nerve injury.

Because Aβ-ES pain therapies were shown to be most effective for alleviating chronic pain with a neuropathic origin, animal models of neuropathic pain are particularly suitable for the exploration of mechanisms underlying pain inhibition by Aβ-ES [15,43,46]. Spinal nerve ligation (SNL) is a common rodent model of neuropathic pain and has been used in studies of neurostimulation pain therapies, such as SCS [17,43,52]. By conducting patch-clamp recording in spinal cord slices from naive and SNL mice, we sought to test the hypothesis that certain frequencies of Aβ-ES may attenuate C-fiber–mediated neurotransmission in SG neurons. Since excitatory and inhibitory interneurons play different roles in modulating spinal pain transmission [48], we further examined whether Aβ-ES differentially modulates their excitability in nerve-injured animals by using transgenic mice in which GABAergic inhibitory interneurons and glutamatergic excitatory neuron can be identified by fluorescence for recording. Our findings suggest that activities in Aβ-fibers may induce prolonged depression of synaptic transmission of noxious afferent inputs in SG neurons.

2. Methods

2.1. Animals and surgery

2.1.1. Animals—Young adult wild-type C57BL/6 mice (5–6 weeks old at the time of electrophysiology recording) and glutamic acid decarboxylase-green fluorescent protein

(GAD-GFP) mice of both sexes were either obtained directly from our vendor (Jackson Laboratory, Bar Harbor, ME) or interbred in our facility from breeding pairs obtained from the vendor. By crossing Rosa26-loxP-STOP-loxP (LSL)-TdTomato mice with vGlut2-Cre mice [4], we generated the offspring vGlut2-Cre:Rosa26-TdTomato mice (vGlut2-Td) to identify glutamatergic excitatory neurons with red fluorescence. All procedures were approved by the Johns Hopkins University Animal Care and Use Committee (Baltimore, MD, USA) as consistent with the National Institutes of Health Guide for the Use of Experimental Animals to ensure minimal animal use and discomfort. Animals received food and water *ad libitum* and were maintained on a 12-hour day–night cycle in isolator cages (maximum of 5 mice/cage).

2.1.2. Spinal nerve ligation (SNL) in mice—Mice of both sexes were anesthetized with 2.0% isoflurane (Abbott Laboratories, North Chicago, IL). The left L4 spinal nerve was exposed and ligated with a 9-0 silk suture and cut distally using methods modified from our previous studies [18,27]. The muscle layer was closed with 6-0 chromic gut suture and the skin closed with metal clips.

2.2. Spinal cord slice preparation

Spinal cord slices were prepared as described in our previous study [27]. A laminectomy was performed in mice deeply anesthetized with 2–3% isoflurane. Then the lumbosacral segment of the spinal cord was rapidly removed with attached dorsal roots and placed in ice-cold, low-sodium Krebs solution (in mM: 95 NaCl, 2.5 KCl, 26 $NaHCO_3$, 1.25 NaH_2PO_4-H_2O, 6 $MgCl_2$, 1.5 $CaCl_2$, 25 glucose, 50 sucrose, 1 kynurenic acid) that was saturated with 95%O_2/5% CO_2. After trimming and mounting the tissue on a tissue slicer (Vibratome VT1200, Leica Biosystems, Buffalo Grove, IL), we prepared 400-μm-thick transverse slices with attached dorsal roots. Dorsal root manipulation was minimized to prevent damage [27]. The slices were then incubated in preoxygenated low-sodium Krebs solution without kynurenic acid. The slices were allowed to recover at 34°C for 40 minutes and then at room temperature for an additional 1 hour before we began the experimental recordings.

2.3. Whole-cell patch-clamp recording in spinal cord slices

Patch-clamp recording was conducted as described in our previous study [27]. Briefly, transverse slices (400 μm) with the dorsal root attached were submerged in a small-volume recording chamber (SD Instruments, San Diego, CA), perfused with room-temperature Krebs solution (in mM: 125 NaCl, 2.5 KCl, 26 $NaHCO_3$, 1.25 $NaH_2PO_4H_2O$, 1 $MgCl_2$, 2 $CaCl_2$, 25 glucose) bubbled with a continuous flow of 95% O_2/5% CO_2, and stabilized with a grid (Ala Scientific, Farmingdale, NY). Whole-cell patch-clamp recording of lamina II cells was carried out under oblique illumination with an Olympus fixed-stage microscope system (BX51, Melville, NY). Data were acquired with pClamp 10 software and a Multiclamp amplifier (Molecular Devices, Sunnyvale, CA). Thin-walled glass pipettes (World Precision Instruments, Sarasota, FL) fabricated with a puller (P1000, Sutter, Novato, CA) had resistances of 3–6 M and were filled with internal saline (in mM: 120 K-gluconate, 20 KCl, 2 $MgCl_2$, 0.5 EGTA, 2 Na_2-ATP, 0.5 Na_2-GTP, and 20 HEPES). The cells were voltage clamped at −70 mV unless otherwise stated. Membrane current signals were

sampled at 10 kHz and low-pass filtered at 2 kHz. Larger bore pipettes filled with Krebs solution were used for dorsal root stimulation.

Spinal cord dorsal horn somatosensory maps undergo postnatal refinement over a critical postnatal period and are completed by the third postnatal week. To avoid developmental changes that may confound data interpretation during early postnatal stages, we have optimized the method for patch clamp recording in young adult mice (5–6 weeks). The gradual postnatal withdrawal of Aβ-fibers from superficial to deeper dorsal horn (laminae III and below) and the maturation of synaptic inputs through C-fibers have mostly completed by this time [3,6,14].

2.4. Compound action potential recording at the dorsal root

To calibrate the Aβ-ES stimulus intensity that selectively activates low-threshold afferent fibers at the dorsal root, we recorded compound action potentials (APs) evoked by graded electrical stimulation (0–1.0 mA, 0.1 ms), as illustrated in the recording configuration (Fig. 1A). The recording pipette was attached to the dorsal root near the dorsal root entry zone. For measuring compound AP conduction velocity (CV) and activation threshold (Fig. 1B), we stimulated the dorsal root three times (Iso-Flex, AMPI, Jerusalem, Israel) at 0.05 Hz with identical intensities and then increased the stimulation intensity. Different waveforms of extracellular compound APs corresponding to Aβ-, Aδ-, and C-fiber activation were distinguished on the basis of the CV and the activation threshold [17,43]. The CV was determined by dividing the distance between the stimulating and recording electrodes by the latency of the peak for each component of the compound AP. To establish the stimulus-response curves for activation of each component, we plotted the amplitude of compound APs, shown as a fraction of the maximum amplitude (MM), against the stimulus intensity (Fig. 1B). The amplitude of the compound AP was measured from the negative to the positive peak voltage.

2.5. Dorsal root stimulation

2.5.1. Aβ-ES—The effectiveness of Aβ-ES pain therapies depends on stimulation frequency. Different frequencies of neurostimulation may have distinct mechanisms of action, as with TENS and electroacupuncture [39,44]. The 2–4 Hz and 50–100 Hz ranges are often used in TENS and SCS, respectively, for pain treatment. Recently, interest has arisen in high-frequency neurostimulation (e.g., kilohertz) for pain treatment [7,35,49]. Therefore, we included 4, 50, and 1000 Hz stimulation for investigational purposes in naïve animals. Because 50 Hz is the most commonly used frequency for Aβ-ES pain therapies in clinic and has been validated in preclinical animal models of neuropathic pain [17,45,47], we focused on testing 50 Hz in the subsequent experiments carried out in SNL mice. To determine the stimulation strength that results predominantly in activation of Aβ-fibers in our setting, we measured the compound APs produced by increasing intensities of electrical stimulation at the dorsal root. Based on the stimulus-response curves of compound APs, for dorsal root Aβ-ES we selected an intensity of 10 μA, which recruited 40% of all Aβ-fibers and maximally avoided the activation of Aδ and C-fibers (Fig. 1B). Aβ-ES was applied via a suction electrode to the attached distal root.

2.5.2. Paired-pulse test stimulation—To evoke postsynaptic currents in SG neurons, we delivered paired-pulse test stimulation to the dorsal root that consisted of two synaptic volleys (500 μA, 0.1 ms) 400 ms apart at a frequency of 0.05 Hz (3 tests/min). This stimulus strength is sufficient to activate C-fibers. We used paired-pulse test stimulation so that we could calculate the paired-pulse ratio (PPR; 2nd amplitude/1st amplitude) [59]. A 0.1 millisecond-long 5 mV depolarizing pulse was used to measure R series and R input; cells were discarded if either of these values changed by more than 20%.

2.6. Drugs

All drugs were applied into the bath (i.e., extracellular) solution. (–)-Bicuculline methochloride and strychnine hydrochloride were dissolved and diluted in extracellular solution. Stock solutions were freshly prepared as instructed by the manufacturer. Drugs were purchased from Sigma-Aldrich (St. Louis, MO) or Tocris Bioscience (Bristol, UK).

2.7. Data analysis

In patch-clamp recording, we determined the peak amplitude of evoked postsynaptic currents and PPR by using custom-written Matlab (Mathworks, Natick, MA) scripts and pClamp software. The evoked postsynaptic current corresponding to C-fiber inputs was distinguished on the basis of the latency and activation threshold. It is known that each spinal cord segment may receive C-fiber inputs from several segmental dorsal roots [37]. Because of multi-segmental projections, branching, and dendrite arborization in the spinal cord, we cannot clearly distinguish the central termini of the injured versus the uninjured dorsal root ganglion neurons at each spinal level in spinal slices of SNL mice. Therefore, we performed the analysis on the combined eEPSC data from L4 and L5 spinal segments in both naïve and nerve-injured mice.

We randomized experiments to the different groups (e.g., naïve and nerve-injured) and blinded the experimenter to the treatments (e.g., drug, nerve injury) to reduce selection and observation bias. After the experiments were completed, no data point was excluded. STATISTICA 6.0 software (StatSoft, Inc., Tulsa, OK) was used to conduct all statistical analyses. The methods for statistical comparisons in each study are given in the figure legends. The Tukey honestly significant difference (HSD) post-hoc test was used to compare specific data points. Bonferroni correction was applied for multiple comparisons. Two-tailed tests were performed, and numerical data are expressed as mean ± SEM; $P < 0.05$ was considered significant in all tests.

3. Results

3.1. Characterization of the extracellular compound APs evoked by graded dorsal root electrical stimulation

Increasing stimulus intensities (0 – 1.0 mA, 0.1 ms) at dorsal root activated Aβ-, Aδ-, and C-fiber components of compound APs progressively (Fig. 1). The fastest component was considered to correspond to Aβ-fiber activation (CV: 5.7 ± 1.2 m/s, n=6). The slower component, referred to as the Aδ-compound AP, usually has a smaller amplitude than the fast Aβ component and was distinguished by a higher threshold and slower CV (1.6 ± 0.3

m/s). The slowest component was considered to correspond to C-fiber activation (CV: 0.7 ± 0.2 m/s, activation threshold > 100 μA). Similar to what has been published before [9], the amplitude of the Aβ-component plateaued at a stimulation intensity of approximately 20 μA, whereas the Aδ-components plateaued at approximately 90 μA. Based on the stimulus-response curves, we selected 10 μA as the intensity for Aβ-ES, because stimulus at this strength (intensity and pulse width) activates roughly 40% of the Aβ-fibers ($42 \pm 14\%$) in the dorsal root and few low-threshold Aδ-fibers ($9 \pm 9.1\%$). This intensity was either comparable to or lower than those used for activation of Aβ-fibers in the dorsal root in previous studies [9,32].

3.2. Aβ-ES inhibits the postsynaptic currents evoked by high-threshold afferent inputs in SG neurons of naïve mice

Because GABA release and GABA-A receptor activation are thought to be important components of the mechanism underlying Aβ-ES analgesia [15,31], we preserved the network of inhibitory neurotransmission in spinal cord slices in the initial set of experiments by excluding GABA-A and glycine receptor antagonists from the bath solution. We examined the effects of Aβ-ES (50 Hz, 10 μA, 0.1 ms, 1 min) on postsynaptic currents evoked by C-fiber inputs in SG neurons. The paired-pulse test stimulation (500 μA, 0.1 ms, 400 ms apart) was applied at the dorsal root at intensities sufficient to activate C-fibers (Fig. 2A, B). After measuring the baseline of evoked postsynaptic currents for 5 minutes, we administered Aβ-ES followed by post-stimulation tests. The peak amplitudes of the 1st C-fiber–evoked postsynaptic current (1st amplitude) to paired-pulse stimulation gradually decreased after Aβ-ES (filled circles, Fig. 2C). The 1st amplitudes during each 5-minute time period after Aβ-ES were averaged and then normalized to the respective baseline values (0–5 minutes before Aβ-ES) for statistical analysis. At 15–20 minutes after Aβ-ES, the 1st amplitude was significantly decreased from pre-stimulation baseline (0.78 ± 0.1 fold, $P<0.05$, n=11; Fig. 2D). The PPR gradually increased after Aβ-ES (Fig. 2E) and was significantly greater than baseline at 15–20 minutes (1.23 ± 0.08 fold, $P<0.05$; Fig. 2F). The access resistance remained largely unchanged during the experiment (data not shown), indicating a stable recording condition.

To determine if GABA-A and glycine receptor activation is involved in this form of synaptic depression induced by 50 Hz Aβ-ES, we next compared the data with that from experiments conducted with GABA-A receptor (bicuculline, 20 μM) and glycinergic receptor (strychnine, 2 μM) antagonists in the bath solution (open circles, Fig. 2C). At 20 minutes after Aβ-ES and in the presence of both antagonists, the 1st amplitude significantly decreased to 0.77 ± 0.07 fold of baseline level (n=6, $P<0.05$; Fig. 2D), and the PPR increased to 1.26 ± 0.12 fold of baseline level ($P<0.05$; Fig. 2F). Thus, including both antagonists did not prevent 50 Hz Aβ-ES from inhibiting C-fiber–evoked postsynaptic currents.

3.3. Evoked excitatory postsynaptic currents (eEPSCs) produced by high-threshold afferent inputs in SG neurons were inhibited by Aβ-ES in a frequency-dependent fashion

To determine the effects of different frequencies of Aβ-ES on regulation of the excitatory synaptic transmission and avoid synaptic current contamination by GABA-A receptor- and

glycine receptor-mediated currents, we specifically recorded eEPSCs in SG neurons (Fig. 3A). We preserved the inhibitory synaptic transmission in spinal cord (i.e., GABA-A and glycine receptor antagonists were omitted from the extracellular solution) by substituting Cl^- with F^- in the intracellular solution [22]. Because F^- will not exit the membrane through activated GABA-A and glycine receptors, replacing Cl^- with F^- in the intracellular solution will substantially diminish GABA-A and glycine current contamination of eEPSCs when membrane potential is at −70 mV [22]. None of the SG neurons recorded exhibited eEPSCs that corresponded to Aδ- or C-fiber input during low-intensity dorsal root stimulation (10 μA, 0.1 ms, Fig. 3B, upper panel). Under these experimental conditions, bath application of antagonists to NMDA (APV, 50 μM) and AMPA (CNQX, 50 μM) receptors completely abolished the eEPSCs evoked by the test stimulus (500 μA, 0.1 ms; Fig. 3B, lower panel), confirming that the evoked currents were solely mediated by glutamate receptors.

To better detect the actions of Aβ-ES, we used a longer induction protocol (5 minutes) than that used in the previous experiment (1 minute). Compared to 1-minute treatment, 5 minutes of 50 Hz Aβ-ES induced a quicker onset and greater inhibition of C-fiber eEPSC (Fig. 3C,D). In naïve mice, the peak amplitudes of the 1st C-fiber eEPSC produced in response to test stimulation progressively decreased from pre-stimulation baseline level after 50 Hz (n=12) and 1000 Hz (n=10) Aβ-ES (10 μA, 0.1 ms, 5 min; Fig. 3C,D). However, 4 Hz Aβ-ES (n=10) was not effective. The amplitudes of the 1st C-fiber eEPSC during each 5-minute period were averaged for analysis (Fig. 3D). The averaged 1st amplitudes were significantly decreased as early as 0–5 minutes after 50 Hz and 1000 Hz Aβ-ES ($P<0.05$), and the inhibition reached a greater peak level by 10–15 minutes after the stimulation. The PPR was significantly increased from baseline at 15–20 minutes after 50 Hz ($P<0.01$), but not 1000 Hz or 4 Hz Aβ-ES (Fig. 3E). Sham stimulation (control, n=12, including 6 naive and 6 SNL mice) did not significantly affect C-fiber eEPSC amplitude or PPR.

3.4. eEPSCs produced by high-threshold afferent inputs in SG neurons were also inhibited by 50 Hz Aβ-ES in nerve-injured mice

Because spinal sensory circuitry may change after nerve injury, and Aβ-ES therapies (e.g., SCS) are often used to alleviate chronic pain with a neuropathic origin, we further investigated the effects of 50 Hz conditioning stimulation in nerve-injured mice. We took advantage of the SNL model, an established surgical model of neuropathic pain that has been used in previous studies to demonstrate the analgesic properties of neurostimulation therapy [17,43,52,54]. We found that 50 Hz Aβ-ES gradually reduced the 1st amplitudes of C-fiber eEPSC in mice at 1–2 weeks after SNL (n=11). The averaged 1st amplitudes were significantly decreased from baseline level from 5–10 minutes until 15–20 minutes after Aβ-ES (Fig. 4A,B), though there was a trend toward the decrease in C-fiber eEPSC being less prominent in nerve-injured mice than in naïve mice. Interestingly, unlike in naïve mice, the PPR did not change significantly from baseline after 50 Hz Aβ-ES in SNL mice (Fig. 4C).

3.5. Aβ-ES of 50 Hz inhibited both monosynaptic and polysynaptic forms of eEPSCs evoked by high-threshold afferent inputs

Monosynaptic and polysynaptic (i.e., through interneurons) forms of eEPSC in dorsal horn neurons in response to high-threshold afferent inputs may be affected differently by

analgesics [40,56]. Therefore, we asked whether Aβ-ES may also differentially modulate these two forms of C-fiber eEPSC in SG neurons. To determine whether the C-fiber eEPSCs are monosynaptic or polysynaptic, we stimulated cells with 20 high-intensity test pulses (500 μA, 0.1 ms) at a frequency of 1 Hz. According to previous studies [24,32], the eEPSC to monosynaptic inputs from C-fibers should have no failures in response to these stimuli (i.e., stimuli fail to evoke a response), though the amplitudes of the eEPSCs may differ (Fig. 5A, left). In contrast, C-fiber eEPSCs evoked by polysynaptic inputs will display prolonged and variable latency and some failures at this frequency (Fig. 5A, right). Compared to baseline values, the 1st amplitudes of both monosynaptic (n=7) and polysynaptic (n=5) C-fiber eEPSCs were decreased after 50 Hz Aβ-ES in naïve mice (Fig. 5B,C). Similarly, both monosynaptic (n=6) and polysynaptic (n=5) C-fiber eEPSCs were decreased after 50 Hz Aβ-ES in SNL mice (Fig. 5D,E).

3.6. Both excitatory and inhibitory interneurons in SG showed decreased excitability after 50 Hz Aβ-ES in nerve-injured mice

Glutamatergic excitatory neurons and GABAergic inhibitory neurons in SG form important local pain modulatory circuitry [48]. Conventionally, it has been difficult to separate and characterize their responses, as the two types of interneurons have similar soma morphology and are interspersed in the superficial layers of the dorsal horn. In GAD-GFP mice, GABAergic dorsal horn neurons can be identified by the expression of enhanced GFP under the control of the GABAergic specific promoter Gad67 [25,34]. In spinal cord slices from GAD-GFP and vGlut2-Td mice, we can clearly identify GABAergic inhibitory and glutamatergic excitatory neurons for recording in SG by green and red fluorescence, respectively (Fig. 6A). Surprisingly, 50 Hz Aβ-ES (10 μA, 0.1 ms, 5 min) inhibited C-fiber eEPSCs in both GAD-GFP–positive (n=11) and vGlut2-Td– positive (n=10) SG neurons in mice at 1–2 weeks after SNL (Fig. 6B).

4. Discussion

The mechanisms underlying pain inhibitory effects of Aβ-fiber stimulation are incompletely understood, despite the burgeoning clinical application of neurostimulation pain therapies. Here, we investigated the synaptic mechanisms of Aβ-ES–induced pain relief by examining its effects on C-fiber–evoked excitatory neurotransmission in SG neurons. We showed that a brief train of Aβ-ES induced a sustained depression of synaptic response to C-fiber inputs in SG neurons in a frequency-dependent fashion. Further, 50 Hz Aβ-ES inhibited both monosynaptic and polysynaptic forms of C-fiber eEPSCs in naive and nerve-injured mice. Notably, both inhibitory and excitatory neurons in SG showed a decrease in C-fiber eEPSC amplitudes after 50 Hz Aβ-ES in nerve-injured mice.

eEPSC measurements are commonly used to assess excitatory neurotransmission in postsynaptic neurons [19,27]. An important feature of Aβ-ES–induced inhibition in SG neurons is that the C-fiber eEPSCs remain depressed for at least 20 minutes after termination of 50 Hz and 1000 Hz Aβ-ES. Our study provides the first electrophysiologic evidence for a prolonged depression of nociceptive transmission in SG neurons following a short period of low-threshold Aβ-fiber stimulation. Classically, the Hebbian protocol for inducing long-term depression in the dorsal horn requires that conditioning electrical

stimulation be applied to activate high-threshold afferent fibers (Aδ- and C-fibers) with concurrent postsynaptic responses in dorsal horn neurons [20,28,38,41]. Unlike this classical protocol, our protocol induced synaptic depression of high-threshold inputs in SG neurons with a much lower stimulus intensity (10 μA), which activates at most a portion of Aβ-fibers in the dorsal root. This intensity is comparable to that used for selective activation of Aβ-fibers in previous studies [9,32]. Further, we did not detect evoked postsynaptic current in any SG neurons that corresponded to activation of Aδ-fibers by dorsal root stimulation at 10 μA. Therefore, the depression of C-fiber eEPSCs was primarily, if not exclusively, a result of Aβ-fiber activation by the conditioning electrical stimulation. Because Aβ-fibers terminate mostly in the deeper laminae, and the recorded SG neurons rarely showed direct synaptic responses to Aβ-fiber inputs, the depression of C-fiber eEPSCs after Aβ-ES may rely on yet unidentified heterosynaptic and network mechanisms. Future studies may examine whether the inhibition of C-fiber eEPSC by Aβ-ES persists when Aδ- and C-fibers are activated concomitantly. For example, does concurrent Aβ-ES inhibit long-term potentiation (LTP) of spinal nociceptive transmission induced by tetanic electrical stimulation of C-fibers or tissue inflammation [42,53]?

Functionally distinct subsets of neurons in SG play different roles in transmitting and modulating pain signals [11,36]. In general, the balance between the pain facilitatory and inhibitory actions in excitatory and inhibitory interneurons fine tunes spinal pain transmission. The gate control theory postulates that stimulation of afferent Aβ-fibers activates GABAergic inhibitory interneurons in dorsal horn, which in turn suppress excitatory neurons and spinal nociceptive transmission [15,30]. Yet, a recent review suggested a contemporary view of gate control and highlighted the complexity of dorsal horn neuronal circuitry that modulates nociceptive transmission [5]. C-fiber eEPSCs in both glutamatergic excitatory and GABAergic inhibitory interneurons were significantly decreased after 50 Hz Aβ-ES in nerve-injured mice. This finding suggests that 50 Hz Aβ-ES failed to induce cell type-selective inhibition of eEPSCs in SG neurons, based on the neurochemical markers that we selected. We limited vGlut2-Td–positive cell selection to SG (lamina II) to maximally avoid recording projection neurons, which are found mostly in lamina I and laminae III-V [48,55]. However, it is possible that subtypes of excitatory (e.g., projection neurons) and inhibitory neurons could have different responses to Aβ-ES. Also, it remains to be examined if Aβ-ES at another frequency (e.g., 1000 Hz), pattern (e.g., burst), or stimulation site (e.g., dorsal column) induces preferential inhibition of excitatory dorsal horn neurons.

The physiologic effect of sustained synaptic depression on nociceptive transmission in SG neurons after Aβ-ES warrants further investigation. Pain relief from Aβ-ES, such as that from TENS and SCS, may briefly outlast the treatment time [17,52]. Currently, the biological basis for these "carryover" pain inhibitory effects is unclear. Previous electrophysiologic studies showed that Aβ-ES decreased wide-dynamic range (WDR) neuronal hyperexcitability in neuropathic rats [17,43,51] and blocked windup in WDR neurons during repetitive noxious stimuli *in vivo* [17]. Further, SCS normalized the LTP in WDR neurons [50]. Windup and LTP reflect short-term and long-lasting neuronal sensitization, respectively, and may share certain mechanisms with those that underlie

persistent pain [17,21,26]. These findings suggest that Aβ-fiber volleys may induce plastic changes in dorsal horn and counteract the spinal neuronal sensitization that underlies persistent pain. However, our current study revealed that excitability in GABAergic inhibitory interneurons is also decreased after 50 Hz Aβ-ES. In general, the compromised inhibitory tone may reduce the pain inhibition of Aβ-ES. Hence, our findings might partially explain why the carryover inhibition of WDR neurons and the effect of Aβ-ES on animal pain behavior *in vivo* are often short-lived [17,43,52]. Nevertheless, a subset of inhibitory interneurons may form synapse connections with another inhibitory interneuron [23,57]; thus it is possible that depression of GABAergic interneurons may paradoxically enhance pain inhibition by disinhibiting other inhibitory interneurons. Additional studies are needed to examine network mechanisms for pain inhibition of Aβ-ES by conducting double patch-clamp recordings in a pair of neurons with synaptic connections, and to investigate the effects of Aβ-ES on projection neurons. The mechanisms that underlie the decreased excitability in GABAergic neurons after 50 Hz Aβ-ES must still be ascertained.

In naïve mice, the decreased C-fiber eEPSC after 50 Hz Aβ-ES was accompanied by an increase in PPR, suggesting that the inhibition of eEPSC may involve a presynaptic site of action, such as a decrease in the probability of excitatory neurotransmitter release from presynaptic terminals [10,19,59]. This finding supports previous data suggesting that SCS analgesia involves presynaptic mechanisms [15,16,45]. Yet, it is unclear why the PPR did not increase significantly after 50 Hz Aβ-ES in nerve-injured mice. Perhaps the PPR did not increase because of substantial anatomical changes in spinal sensory circuitry after peripheral nerve injury, such as changes in sensory mapping and excitatory synaptic transmission in lamina II [24,33]. For example, the excitatory synaptic drive onto putative inhibitory neurons in SG may decrease after nerve injury and lead to decreased inhibition [1]. Further, nerve injury may differentially affect the presynaptic mechanisms of excitatory and inhibitory neurotransmission in SG neurons [58]. The neurochemical and neurophysiologic changes after nerve injury may thereby alter the mechanisms by which Aβ-ES modulates C-fiber eEPSC. The respective pre- and postsynaptic mechanisms and pathways by which Aβ-ES inhibits C-fiber eEPSCs in different subsets of SG neurons, especially after nerve injury, warrant additional studies.

A subgroup of GABAergic interneurons in dorsal horn are activated by convergent Aβ-fiber inputs [9]. The increased extracellular GABA level, which induces neuronal inhibition, may exceed the duration of Aβ-ES (e.g., SCS), but only for a short time [8]. However, in our study, the inhibition of C-fiber eEPSC in both excitatory and inhibitory interneurons by Aβ-ES developed gradually and peaked at 15–20 minutes after Aβ-ES was complete. Several factors could cause the different studies to have different time courses. First, the descending modulation that may be activated by Aβ-ES *in vivo* is lost during the recording of SG neurons in spinal slices. Second, the effect of *in vivo* Aβ-ES on deep WDR neurons reflects the combined actions on afferent terminals, superficial neurons, deep neurons, and interneurons in contact with them. Thus, the intrinsic spinal network mechanisms by which Aβ-ES modulates superficial SG neurons and deep WDR neurons may be different. Third, we found that blocking fast inhibitory neurotransmission mediated by GABA-A receptors and glycine receptors, which may be important to pain gate-control, did not preclude the

Author Manuscript

prolonged synaptic depression induced by 50 Hz Aβ-ES. The neurochemical mechanisms that underlie the sustained synaptic depression in excitatory and inhibitory neurons after Aβ-ES warrant future studies.

Low frequency (e.g., 2–4 Hz) TENS induces pain inhibition, but in our study, 4 Hz Aβ-ES did not inhibit C-fiber eEPSCs in naïve animals. This finding suggests that the mechanisms underlying pain inhibition by low- and high-frequency Aβ-ES may differ. It remains to be examined if 4 Hz Aβ-ES inhibits C-fiber eEPSCs in nerve-injured animals. Descending modulation from supraspinal structures significantly affects dorsal horn neurons, including SG neurons [48]. Pain inhibition from Aβ-ES *in vivo* involves both spinal and supraspinal mechanisms [2,46]. Because tonic descending modulation could influence the direction (e.g., potentiation or depression) of plastic changes in C-fiber–mediated synaptic transmission [28], our current findings may not fully reflect the actions of Aβ-ES that occur in intact animal preparations. Nevertheless, the prolonged synaptic depression, especially in excitatory neurons, may represent another segmental cellular mechanism that contributes to pain inhibition by Aβ-ES therapies. Our study may inspire the exploration of additional spinal substrates that underlie the therapeutic actions of neurostimulation techniques in defined neuronal populations, such as using transgenic mice that express fluorescent proteins in functionally distinct subsets of dorsal horn neurons [34]. The knowledge obtained from these mechanistic studies may enable us to improve the clinical efficacy of neurostimulation pain therapy in the future.

Acknowledgments

References

1. Balasubramanyan S, Stemkowski PL, Stebbing MJ, Smith PA. Sciatic chronic constriction injury produces cell-type-specific changes in the electrophysiological properties of rat substantia gelatinosa neurons. J Neurophysiol. 2006; 96:579–90. [PubMed: 16611846]

2. Barchini J, Tchachaghian S, Shamaa F, Jabbur SJ, Meyerson BA, Song Z, Linderoth B, Saade NE. Spinal segmental and supraspinal mechanisms underlying the pain-relieving effects of spinal cord stimulation: an experimental study in a rat model of neuropathy. Neuroscience. 2012; 215:196–208. [PubMed: 22548781]

3. Beggs S, Torsney C, Drew LJ, Fitzgerald M. The postnatal reorganization of primary afferent input and dorsal horn cell receptive fields in the rat spinal cord is an activity-dependent process. Eur J Neurosci. 2002; 16:1249–58. [PubMed: 12405985]

4. Borgius L, Restrepo CE, Leao RN, Saleh N, Kiehn O. A transgenic mouse line for molecular genetic analysis of excitatory glutamatergic neurons. Mol Cell Neurosci. 2010; 45:245–57. [PubMed: 20600924]

5. Braz J, Solorzano C, Wang X, Basbaum AI. Transmitting pain and itch messages: a contemporary view of the spinal cord circuits that generate gate control. Neuron. 2014; 82:522–36. [PubMed: 24811377]

6. Cabanes C, de Lopez AM, Viana F, Belmonte C. Postnatal changes in membrane properties of mice trigeminal ganglion neurons. J Neurophysiol. 2002; 87:2398–407. [PubMed: 11976377]

7. Cuellar JM, Alataris K, Walker A, Yeomans DC, Antognini JF. Effect of High-Frequency Alternating Current on Spinal Afferent Nociceptive Transmission. Neuromodulation. 2012

8. Cui JG, O'Connor WT, Ungerstedt U, Linderoth B, Meyerson BA. Spinal cord stimulation attenuates augmented dorsal horn release of excitatory amino acids in mononeuropathy via a GABAergic mechanism. Pain. 1997; 73:87–95. [PubMed: 9414060]

9. Daniele CA, MacDermott AB. Low-threshold primary afferent drive onto GABAergic interneurons in the superficial dorsal horn of the mouse. J Neurosci. 2009; 29:686–95. [PubMed: 19158295]

10. Dobrunz LE, Stevens CF. Heterogeneity of release probability, facilitation, and depletion at central synapses. Neuron. 1997; 18:995–1008. [PubMed: 9208866]

11. Dubuisson D. Effect of dorsal-column stimulation on gelatinosa and marginal neurons of cat spinal cord. J Neurosurg. 1989; 70:257–65. [PubMed: 2913223]

12. Falowski S, Sharan A. A review on spinal cord stimulation. J Neurosurg Sci. 2012; 56:287–98. [PubMed: 23111289]

13. Finnerup NB, Sindrup SH, Jensen TS. Recent advances in pharmacological treatment of neuropathic pain. F1000 Med Rep. 2010; 2:52. [PubMed: 21170362]

14. Fitzgerald M, Butcher T, Shortland P. Developmental changes in the laminar termination of A fibre cutaneous sensory afferents in the rat spinal cord dorsal horn. J Comp Neurol. 1994; 348:225–33. [PubMed: 7814689]

15. Foreman RD, Linderoth B. Neural mechanisms of spinal cord stimulation. Int Rev Neurobiol. 2012; 107:87–119. [PubMed: 23206679]

16. Guan Y. Spinal cord stimulation: neurophysiological and neurochemical mechanisms of action. Curr Pain Headache Rep. 2012; 16:217–25. [PubMed: 22399391]

17. Guan Y, Wacnik PW, Yang F, Carteret AF, Chung CY, Meyer RA, Raja SN. Spinal cord stimulation-induced analgesia: electrical stimulation of dorsal column and dorsal roots attenuates dorsal horn neuronal excitability in neuropathic rats. Anesthesiology. 2010; 113:1392–405. [PubMed: 21068658]

18. He SQ, Li Z, Chu YX, Han L, Xu Q, Li M, Yang F, Liu Q, Tang Z, Wang Y, Hin N, Tsukamoto T, Slusher B, Tiwari V, Shechter R, Wei F, Raja SN, Dong X, Guan Y. MrgC agonism at central terminals of primary sensory neurons inhibits neuropathic pain. Pain. 2014; 155:534–44. [PubMed: 24333779]

19. Heinke B, Gingl E, Sandkuhler J. Multiple targets of mu-opioid receptor-mediated presynaptic inhibition at primary afferent Adelta- and C-fibers. J Neurosci. 2011; 31:1313–22. [PubMed: 21273416]

20. Ikeda H, Kiritoshi T, Murase K. Synaptic plasticity in the spinal dorsal horn. Neurosci Res. 2009; 64:133–6. [PubMed: 19428692]

21. Ji RR, Kohno T, Moore KA, Woolf CJ. Central sensitization and LTP: do pain and memory share similar mechanisms? Trends Neurosci. 2003; 26:696–705. [PubMed: 14624855]

22. Kato A, Punnakkal P, Pernia-Andrade AJ, von SC, Sharopov S, Nyilas R, Katona I, Zeilhofer HU. Endocannabinoid-dependent plasticity at spinal nociceptor synapses. J Physiol. 2012; 590:4717–33. [PubMed: 22826132]

23. Kato G, Kawasaki Y, Ji RR, Strassman AM. Differential wiring of local excitatory and inhibitory synaptic inputs to islet cells in rat spinal lamina II demonstrated by laser scanning photostimulation. J Physiol. 2007; 580:815–33. [PubMed: 17289782]

24. Kohno T, Moore KA, Baba H, Woolf CJ. Peripheral nerve injury alters excitatory synaptic transmission in lamina II of the rat dorsal horn. J Physiol. 2003; 548:131–8. [PubMed: 12576493]

25. Li J, Blankenship ML, Baccei ML. Deficits in glycinergic inhibition within adult spinal nociceptive circuits after neonatal tissue damage. Pain. 2013; 154:1129–39. [PubMed: 23639821]

26. Li J, Simone DA, Larson AA. Windup leads to characteristics of central sensitization. Pain. 1999; 79:75–82. [PubMed: 9928779]

27. Li Z, He SQ, Xu Q, Yang F, Tiwari V, Liu Q, Tang Z, Han L, Chu YX, Wang Y, Hin N, Tsukamoto T, Slusher B, Guan X, Wei F, Raja SN, Dong X, Guan Y. Activation of MrgC receptor inhibits N-type calcium channels in small-diameter primary sensory neurons in mice. Pain. 2014

28. Liu XG, Morton CR, Azkue JJ, Zimmermann M, Sandkuhler J. Long-term depression of C-fibre-evoked spinal field potentials by stimulation of primary afferent A delta-fibres in the adult rat. Eur J Neurosci. 1998; 10:3069–75. [PubMed: 9786201]

29. Luo C, Kuner T, Kuner R. Synaptic plasticity in pathological pain. Trends Neurosci. 2014; 37:343–55. [PubMed: 24833289]

30. Melzack R, Wall PD. Pain mechanisms: a new theory. Science. 1965; 150:971–9. [PubMed: 5320816]

31. Meyerson BA, Linderoth B. Mode of action of spinal cord stimulation in neuropathic pain. J Pain Symptom Manage. 2006; 31:S6–12. [PubMed: 16647596]

32. Nakatsuka T, Ataka T, Kumamoto E, Tamaki T, Yoshimura M. Alteration in synaptic inputs through C-afferent fibers to substantia gelatinosa neurons of the rat spinal dorsal horn during postnatal development. Neuroscience. 2000; 99:549–56. [PubMed: 11029546]

33. Okamoto M, Baba H, Goldstein PA, Higashi H, Shimoji K, Yoshimura M. Functional reorganization of sensory pathways in the rat spinal dorsal horn following peripheral nerve injury. J Physiol. 2001; 532:241–50. [PubMed: 11283238]

34. Oliva AA Jr, Jiang M, Lam T, Smith KL, Swann JW. Novel hippocampal interneuronal subtypes identified using transgenic mice that express green fluorescent protein in GABAergic interneurons. J Neurosci. 2000; 20:3354–68. [PubMed: 10777798]

35. Perruchoud C, Eldabe S, Batterham AM, Madzinga G, Brookes M, Durrer A, Rosato M, Bovet N, West S, Bovy M, Rutschmann B, Gulve A, Garner F, Buchser E. Analgesic Efficacy of High-Frequency Spinal Cord Stimulation: A Randomized Double-Blind Placebo-Controlled Study. Neuromodulation. 2013

36. Petersen-Zeitz KR, Basbaum AI. Second messengers, the substantia gelatinosa and injury-induced persistent pain. 44 632. Pain. 1999; (Suppl 6):S5–12. [PubMed: 10491967]

37. Pinto V, Derkach VA, Safronov BV. Role of TTX-sensitive and TTX-resistant sodium channels in Adelta- and C-fiber conduction and synaptic transmission. J Neurophysiol. 2008; 99:617–28. [PubMed: 18057109]

38. Randic M, Jiang MC, Cerne R. Long-term potentiation and long-term depression of primary afferent neurotransmission in the rat spinal cord. J Neurosci. 1993; 13:5228–41. [PubMed: 8254370]

39. Romita VV, Suk A, Henry JL. Parametric studies on electroacupuncture-like stimulation in a rat model: effects of intensity, frequency, and duration of stimulation on evoked antinociception. Brain Res Bull. 1997; 42:289–96. [PubMed: 9043715]

40. Ruscheweyh R, Sandkuhler J. Differential actions of spinal analgesics on mono-versus polysynaptic Adelta-fibre-evoked field potentials in superficial spinal dorsal horn in vitro. Pain. 2000; 88:97–108. [PubMed: 11098104]

41. Sandkuhler J, Chen JG, Cheng G, Randic M. Low-frequency stimulation of afferent Adelta-fibers induces long-term depression at primary afferent synapses with substantia gelatinosa neurons in the rat. J Neurosci. 1997; 17:6483–91. [PubMed: 9236256]

42. Sandkuhler J, Gruber-Schoffnegger D. Hyperalgesia by synaptic long-term potentiation (LTP): an update. Curr Opin Pharmacol. 2012; 12:18–27. [PubMed: 22078436]

43. Shechter R, Yang F, Xu Q, Cheong YK, He SQ, Sdrulla A, Carteret AF, Wacnik PW, Dong X, Meyer RA, Raja SN, Guan Y. Conventional and Kilohertz-frequency Spinal Cord Stimulation Produces Intensity- and Frequency-dependent Inhibition of Mechanical Hypersensitivity in a Rat Model of Neuropathic Pain. Anesthesiology. 2013; 119:422–32. [PubMed: 23880991]

44. Sluka KA, Judge MA, McColley MM, Reveiz PM, Taylor BM. Low frequency TENS is less effective than high frequency TENS at reducing inflammation-induced hyperalgesia in morphine-tolerant rats. Eur J Pain. 2000; 4:185–93. [PubMed: 10957699]

45. Smits H, van KM, Holsheimer J, Joosten EA. Experimental spinal cord stimulation and neuropathic pain: mechanism of action, technical aspects, and effectiveness. Pain Pract. 2013; 13:154–68. [PubMed: 22780956]

46. Song Z, Ansah OB, Meyerson BA, Pertovaara A, Linderoth B. The rostroventromedial medulla is engaged in the effects of spinal cord stimulation in a rodent model of neuropathic pain. Neuroscience. 2013; 247:134–44. [PubMed: 23711584]

47. Song Z, Meyerson BA, Linderoth B. Spinal 5-HT receptors that contribute to the pain-relieving effects of spinal cord stimulation in a rat model of neuropathy. Pain. 2011; 152:1666–73. [PubMed: 21514998]

48. Todd AJ. Neuronal circuitry for pain processing in the dorsal horn. Nat Rev Neurosci. 2010; 11:823–36. [PubMed: 21068766]

49. Van Buyten JP, Al-Kaisy A, Smet I, Palmisani S, Smith T. High-frequency spinal cord stimulation for the treatment of chronic back pain patients: results of a prospective multicenter European clinical study. Neuromodulation. 2013; 16:59–65. [PubMed: 23199157]

50. Wallin J, Fiska A, Tjolsen A, Linderoth B, Hole K. Spinal cord stimulation inhibits long-term potentiation of spinal wide dynamic range neurons. Brain Res. 2003; 973:39–43. [PubMed: 12729951]

51. Yakhnitsa V, Linderoth B, Meyerson BA. Spinal cord stimulation attenuates dorsal horn neuronal hyperexcitability in a rat model of mononeuropathy. Pain. 1999; 79:223–33. [PubMed: 10068168]

52. Yang F, Carteret AF, Wacnik PW, Chung CY, Xing L, Dong X, Meyer RA, Raja SN, Guan Y. Bipolar spinal cord stimulation attenuates mechanical hypersensitivity at an intensity that activates a small portion of A-fiber afferents in spinal nerve-injured rats. Neuroscience. 2011; 199:470–80. [PubMed: 22001681]

53. Yang F, Guo J, Sun WL, Liu FY, Cai J, Xing GG, Wan Y. The induction of long-term potentiation in spinal dorsal horn after peripheral nociceptive stimulation and contribution of spinal TRPV1 in rats. Neuroscience. 2014; 269:59–66. [PubMed: 24680883]

54. Yang F, Xu Q, Cheong YK, Shechter R, Sdrulla A, He SQ, Tiwari V, Dong X, Wacnik PW, Meyer R, Raja SN, Guan Y. Comparison of intensity-dependent inhibition of spinal wide-dynamic range neurons by dorsal column and peripheral nerve stimulation in a rat model of neuropathic pain. Eur J Pain. 2014

55. Yasaka T, Tiong SY, Hughes DI, Riddell JS, Todd AJ. Populations of inhibitory and excitatory interneurons in lamina II of the adult rat spinal dorsal horn revealed by a combined electrophysiological and anatomical approach. Pain. 2010; 151:475–88. [PubMed: 20817353]

56. Zhang HM, Chen SR, Pan HL. Regulation of glutamate release from primary afferents and interneurons in the spinal cord by muscarinic receptor subtypes. J Neurophysiol. 2007; 97:102–9. [PubMed: 17050831]

57. Zheng J, Lu Y, Perl ER. Inhibitory neurones of the spinal substantia gelatinosa mediate interaction of signals from primary afferents. J Physiol. 2010; 588:2065–75. [PubMed: 20403977]

58. Zhou C, Luo ZD. Electrophysiological characterization of spinal neuron sensitization by elevated calcium channel alpha-2-delta-1 subunit protein. Eur J Pain. 2014; 18:649–58. [PubMed: 24151064]

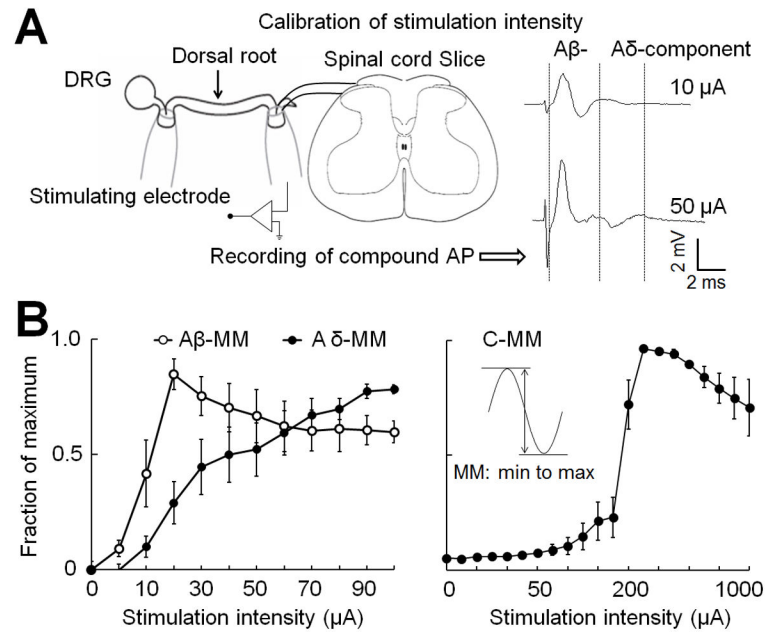59. Zucker RS, Regehr WG. Short-term synaptic plasticity. Annu Rev Physiol. 2002; 64:355–405. [PubMed: 11826273]

Fig. 1. Calibrating the intensity of dorsal root electrical stimulation

(A) Left: Configuration for extracellular recording of compound action potentials (APs) produced by graded dorsal root electrical stimulation. In a transverse spinal cord slice, the stimulating electrode was placed distally on the dorsal root, and the compound AP recording electrode was placed close to the dorsal root entry zone. Right: Examples of increasing stimulus intensities of dorsal root stimulation that activated Aβ- and Aδ-fiber components of compound APs. DRG, dorsal root ganglion. **(B)** The stimulus response curves were established by plotting the amplitude of the compound APs, shown as a fraction of the maximum amplitude (MM, inset), against the increasing stimulus intensity (0–1.0 mA, 0.1 ms). The Aβ-compound AP amplitude plateaued first, followed by the Aδ-component (left), and then, at much higher intensities (>100 μA), the C-component (right). Data are expressed as mean ± SEM in B.
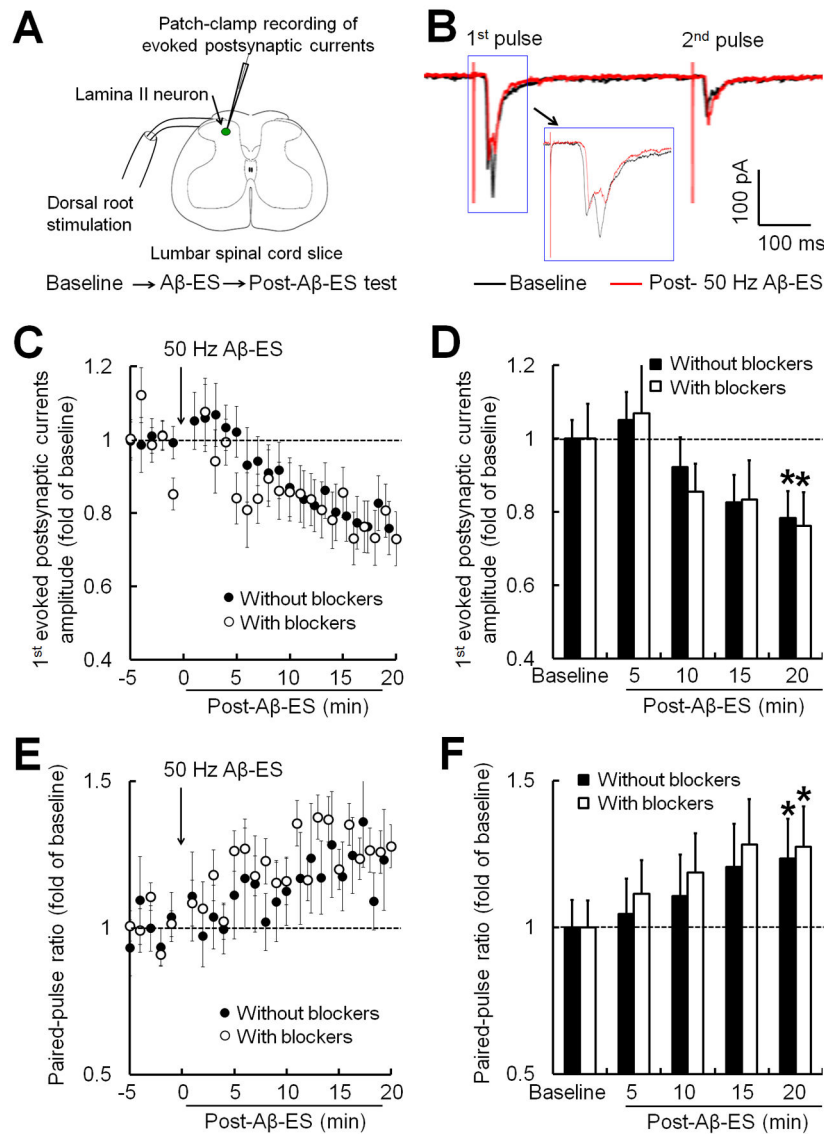
Fig. 2. Electrical stimulation of Aβ-fibers in the dorsal root inhibits evoked postsynaptic currents in substantia gelatinosa neurons

(A) Configuration for whole-cell patch-clamp recording in a substantia gelatinosa (SG) neuron during dorsal root stimulation in a spinal cord slice. First, a baseline recording was obtained (5 min). Then electrical stimulation of Aβ-fibers (Aβ-ES, 50 Hz, 10 μA, 0.1 ms, 1 min) was administered to the ipsilateral dorsal root. Finally, post-stimulation tests were obtained for 20 minutes after stimulation. **(B)** Representative traces of postsynaptic currents in an SG neuron evoked in response to paired-pulse test stimulation (500 μA, 0.1 ms, 400 ms apart) before (black) and after (red) Aβ-ES. The traces of 1st evoked postsynaptic currents in response to high-threshold afferent (i.e., C-fiber) inputs are also shown on a smaller timescale (inset). **(C)** Time course of amplitudes of the 1st C-fiber–evoked postsynaptic currents in SG neurons of naïve mice before and after Aβ-ES. The 50 Hz Aβ-ES induced progressive inhibition of C-fiber–evoked postsynaptic currents in the presence (n=6) and absence of GABA-A receptor (bicuculline, 20 μM) and glycine receptor (strychnine, 2 μM)

blockers (bath application, n=11). **(D)** The amplitudes of the 1st C-fiber–evoked postsynaptic currents during each 5-minute period were averaged for analysis (one-way repeated measures ANOVA). **(E)** Time course of paired-pulse ratio (2nd amplitude / 1st amplitude) before and after Aβ-ES. **(F)** The averaged paired-pulse ratios were increased at 15–20 minutes after Aβ-ES in both groups (one-way repeated measures ANOVA). Data are expressed as mean ± SEM (C-F). *P<0.05 as compared with the baseline.
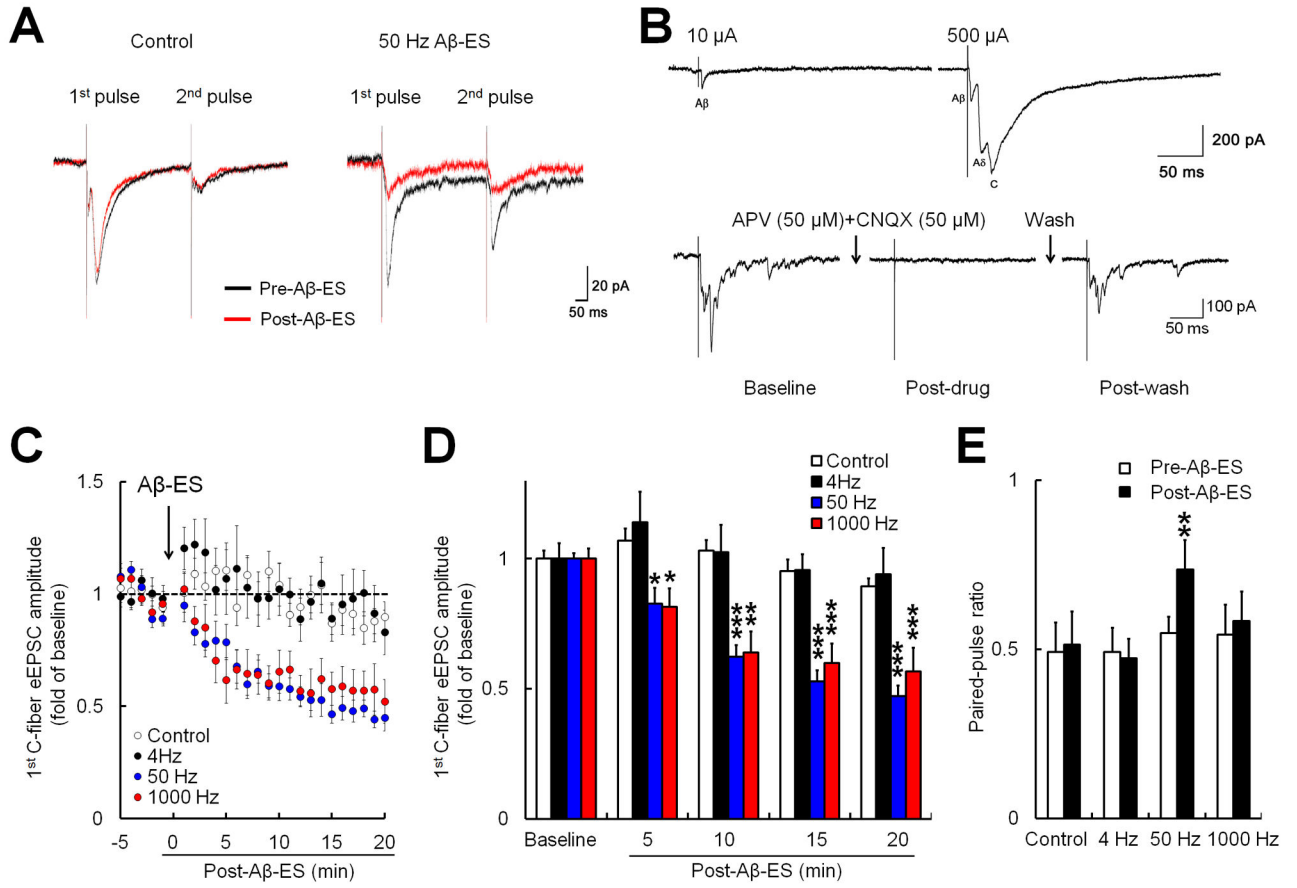
Fig. 3. Electrical stimulation of Aβ-fibers induces frequency-dependent inhibition of evoked excitatory postsynaptic currents (eEPSCs) produced by high-threshold afferent fiber inputs in substantia gelatinosa (SG) neurons

(A) Representative traces of eEPSCs in SG neurons. The eEPSCs were produced by paired-pulse test stimulation (500 μA, 0.1 ms, 400 ms apart) before (black) and after (red) sham stimulation (control) and 50 Hz electrical stimulation of the dorsal root at Aβ-intensity (Aβ-ES, 10 μA, 0.1 ms, 5 min). **(B)** Upper panel: Example of an SG neuron that showed only Aβ-fiber eEPSCs in response to a 10 μA test stimulus but Aβ-, Aδ-, and C-fiber eEPSCs in response to a high-intensity (500 μA) test stimulus. Lower panel: eEPSCs evoked by a high-intensity test stimulus were completely blocked by glutamate receptor antagonists (APV, 50 μM; CNQX, 50 μM). **(C)** Time-dependent changes in the amplitudes of the 1st C-fiber eEPSCs after Aβ-ES in naïve mice (4 Hz: n=10, 50 Hz: n=12, 1000 Hz: n=10). Data from sham stimulation (control) in naïve and nerve-injured mice were combined for analysis (n=12). **(D)** The amplitudes of the 1st C-fiber eEPSC during each 5-minute period were averaged for analysis (one-way repeated measures ANOVA). **(E)** The paired-pulse ratio (2nd amplitude / 1st amplitude) was significantly increased from baseline at 15–20 minutes after 50 Hz Aβ-ES (paired t-test). Data are expressed as mean ± SEM (C-E). $*P<0.05$, $**P<0.01$, $***P<0.001$ as compared with the baseline.
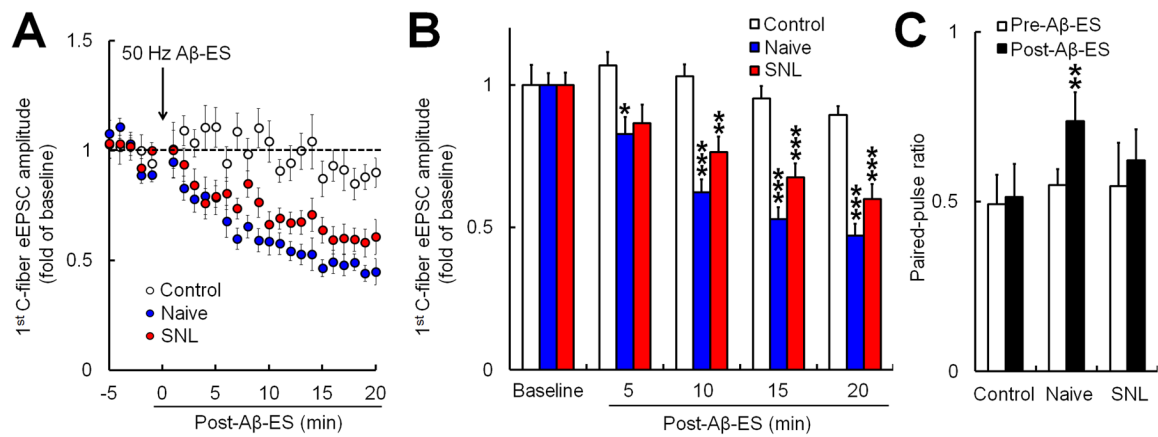
Fig. 4. Electrical stimulation of Aβ-fibers inhibits evoked excitatory postsynaptic currents (eEPSCs) produced by high-threshold afferent fiber inputs in both naive and nerve-injured mice (A) Time-dependent changes in the amplitudes of the 1st C-fiber eEPSCs after Aβ-ES in naïve mice (n=12) and mice that underwent spinal nerve ligation (SNL, n=11). Data from sham stimulation (control) in naïve and SNL mice were combined for analysis (n=12). (B) The amplitudes of the 1st C-fiber eEPSC during each 5-minute period were averaged for analysis in each group (one-way repeated measures ANOVA). (C) The paired-pulse ratio (2nd amplitude / 1st amplitude) at 15–20 minutes after Aβ-ES was significantly increased from baseline (paired t-test) in naïve mice, but not in SNL mice. Data are expressed as mean ± SEM. *$P<0.05$, **$P<0.01$, ***$P<0.001$ as compared with the baseline.
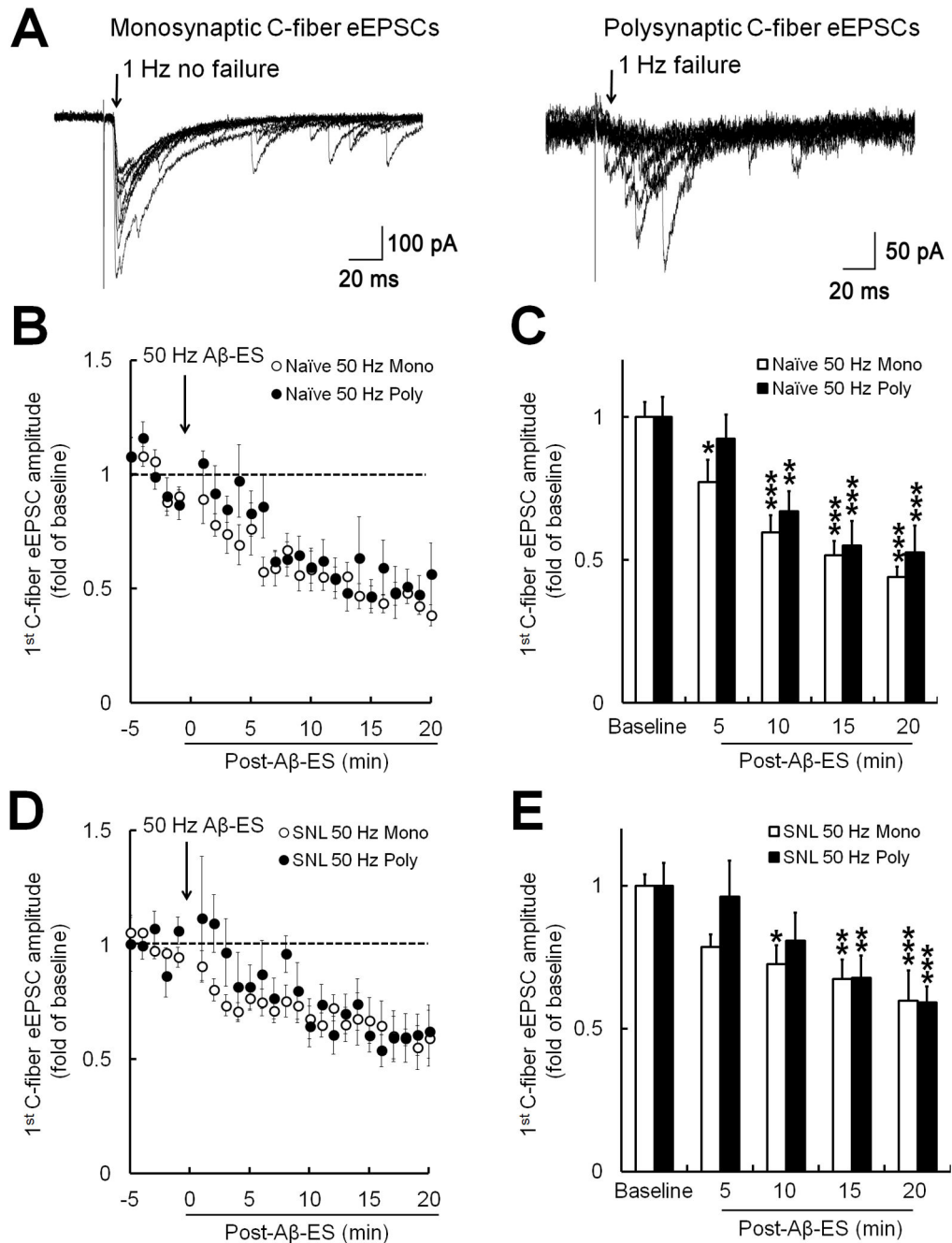
Fig. 5. Dorsal root stimulation inhibits both monosynaptic and polysynaptic forms of evoked excitatory postsynaptic currents (eEPSCs) produced by high-threshold afferent fiber inputs
(**A**) Examples of monosynaptic (left) and polysynaptic (right) eEPSCs produced by high-threshold afferent fiber (i.e., C-fiber) inputs in substantia gelatinosa (SG) neurons. The C-fiber eEPSCs were judged to be monosynaptic if no failures occurred during 20 test pulses (500 μA, 0.1 ms) applied to the dorsal root at 1 Hz, despite variability of C-fiber eEPSC amplitude (left). The eEPSCs of the 20 traces are superimposed. (**B**) In naïve mice, 50 Hz Aβ-ES (10 μA, 0.1 ms, 5 min) at the dorsal root reduced the 1st C-fiber eEPSC in SG

neurons that showed monosynaptic (n=7) and polysynaptic (n=5) components of C-fiber eEPSCs. **(C)** The amplitudes of the 1st C-fiber eEPSCs during each 5-minute period in naïve mice were averaged for analysis (one-way repeated measures ANOVA). **(D)** Changes in the 1st C-fiber eEPSCs in SNL mice after Aβ-ES in SG neurons that showed monosynaptic (n=6) and polysynaptic components (n=5). **(E)** The amplitudes of the 1st C-fiber eEPSCs during each 5-minute period in SNL rats were averaged for analysis (one-way repeated measures ANOVA). Data are expressed as mean ± SEM (B–E). *$P<0.05$, **$P<0.01$, ***$P<0.001$ as compared with the baseline.
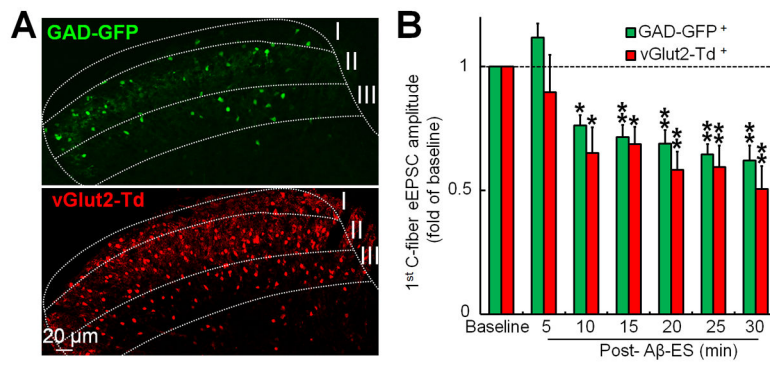
Fig. 6. Effects of 50 Hz electrical stimulation of Aβ-fibers on inhibitory and excitatory dorsal horn neurons

(A) Confocal images of spinal cord slices from GAD-GFP and vGlut2-Td mice. GABAergic inhibitory interneurons can be identified by green fluorescence in slices from GAD-GFP mice, and glutamatergic excitatory neurons can be identified by red fluorescence in slices from vGlut2-Td mice. **(B)** Aβ-ES (50 Hz, 10 μA, 0.1 ms, 5 min) induces prolonged inhibition of C-fiber eEPSCs in both GAD-GFP–positive (+, n=11) and vGlut2-Td–positive (n=10) neurons in mice with spinal nerve ligation (one-way repeated measures ANOVA). Data are expressed as mean ± SEM. *P <0.05, **P <0.01 as compared with the baseline.